RADIATION RESEARCH **185**, 000–000 (2016)
0033-7587/16 $15.00

DOI: 10.1667/RR14072.1

Localized External Beam Radiation Therapy (EBRT) to the Pelvis Induces Systemic IL-1Beta and TNF-Alpha Production: Role of the TNF-Alpha Signaling in EBRT-Induced Fatigue

Tasha L. McDonald,[a,1] Arthur Y. Hung,[a] Charles R. Thomas, Jr. Jr.[a] and Lisa J. Wood[b,2]

[a] *Department of Radiation Medicine, Oregon Health and Science University, Portland, Oregon; and* [b] *Amelia Peabody Professor for Nursing Research, MGH Institute of Health Professions, School of Nursing, Boston, Massachusetts*

McDonald, T. L., Hung, A. Y., Thomas, C. R. and Wood, L. J. Localized External Beam Radiation Therapy (EBRT) to the Pelvis Induces Systemic IL-1beta and TNF-Alpha Production: Role of the TNF-Alpha Signaling in EBRT-Induced Fatigue. *Radiat. Res*. 185, 000–000 (2016).

Prostate cancer patients undergoing localized external beam radiation therapy (EBRT) can experience a progressive increase in fatigue, which can affect physical functioning and quality of life. The purpose of this study was to develop a mouse EBRT prostate cancer treatment model with which to determine the role of pro-inflammatory cytokines in the genesis of EBRT-related fatigue. We assessed voluntary wheel-running activity (VWRA) as a proxy for fatigue, food intake and body weight in male C57BL/6 mice undergoing EBRT to the pelvis. In the first experiment, anesthetized male C57BL/6 mice underwent fractionated EBRT to the pelvis for a total dose of 68.2 Gy, thereby mimicking a clinically relevant therapeutic dose and frequency. The day after the last treatment, levels of IL-1β and TNF-α in plasma along with mRNA levels in liver, colon and whole brain were measured. EBRT-induced fatigue resulted in reduced body weight, diminished food intake, and increased plasma and tissue levels of IL-1β and TNF-α. In a follow-up experiment, we used TNF-α-deficient mice to further delineate the role of TNF-α signaling in EBRT-induced sickness behavior. EBRT-induced changes in fatigue, food intake and body weight were no different between TNF-α deficient mice and their wild-type counterparts. Taken together our data demonstrate that a clinically relevant localized irradiation of the pelvis induces a systemic IL-1β and TNF-α response and sickness behavior in mice, but the TNF-α signaling pathway alone does not independently mediate these effects.

INTRODUCTION

Men undergoing localized external beam radiation therapy (EBRT) for early stage prostate cancer can experience increasing levels of fatigue during treatment that reduces quality of life, physical functioning and long-term overall health (*1–7*). Although fatigue can exist prior to the start of treatment, it tends to increase during treatment and peak towards the end of a treatment course (*8*). In the majority of prostate cancer survivors fatigue gradually declines to pre-treatment levels. However, in a small percentage of prostate cancer survivors, fatigue can persist for several months or years post-treatment (*1, 2, 9*). Several treatment-related factors may contribute to the subjective burden of fatigue in prostate cancer survivors, including the volume of tissue treated and the severity of gastrointestinal and urinary symptoms (*7, 8, 10, 11*). EBRT injures malignant and nonmalignant cells alike. The release of intracellular molecules from injured cells triggers an innate immune response characterized by the upregulation of the pro-inflammatory cytokines IL-1β and TNF-α (*12*). In addition to coordinating tissue repair mechanisms, these cytokines trigger a set of behavioral changes that are hypothesized to promote recovery (*13, 14*). Collectively these behavioral changes are termed ''sickness behavior'' of which fatigue or lethargy is a predominant symptom. In rodent models of sickness behavior, change in locomotor activity, i.e., reduced ambulatory activity or voluntary wheel-running activity (VWRA), a sensitive objective marker of sickness, is often used as a proxy for fatigue (*15*). Using these models, inflammation-induced lethargy was found to be due to hypofunction of hypothalamic orexin-secreting neurons (*16*). We and others have used rodent models of sickness behavior to investigate the molecular mechanisms underlying cancer chemotherapy-related fatigue (*17–21*). In our recent studies we found that the acute fatigue that occurs immediately after chemotherapy administration is caused by orexin neuron hypofunction (*17*). This finding supports the hypothesis that acute cancer chemotherapy-related fatigue may be the same as the fatigue in sickness behavior (*22*). It is not known whether EBRT-

[1] Current address: Salem Hospital Radiation Oncology, Salem Cancer Institute, Salem, OR.

[2] Address for correspondence: MGH Institute of Health Professions, School of Nursing, 36 1st Avenue, Charlestown Navy Yard, Boston, MA, 20219; email: ljwood@mghihp.edu.

related fatigue is caused by the same mechanism. Increases in circulating levels of inflammatory cytokines and chemokines have been observed in men undergoing radiation therapy for prostate cancer (*23*). Yet, few clinical studies have examined the relationship between inflammatory cytokines and fatigue in men undergoing localized EBRT for prostate cancer. Greenberg *et al*. were the first to examine changes in IL-1β and fatigue in men undergoing EBRT (*24*). They observed a concurrent increase in circulating IL-1β and fatigue level during treatment (*24*). In a more recent study the EBRT-related increase in fatigue was not associated with a similar increase in circulating IL-1β, TNF-α, IL-6, IL-10 and IL-4 (*25*). We hypothesized that modeling EBRT-related fatigue in animal models would clarify the specific role of inflammatory cytokines in the genesis of EBRT-related fatigue. The purpose of the current study was to develop a clinically relevant mouse model of localized EBRT with which to determine the specific role of inflammatory cytokines in the genesis of EBRT-related fatigue.

MATERIALS AND METHODS

Mice

All animal procedures were performed according to protocols that have been approved by the Institutional Animal Care and Use Committee at Oregon Health and Science University. Wild-type C57BL/6 male mice, 10–12 weeks old and mice lacking TNF-α were purchased from Jackson Laboratories (cat. no. 00664 and B6;129S6-*Tnf*^{tm1Gkl}/J; cat. no. 005540, respectively; Bar Harbor, ME). TNF-deficient mice lack TNF-α in all tissues, are viable and fertile and show no phenotypic anomalies. This strain shows a blunted immune response to immune challenge and complete resistance to endotoxin-induced death (*26*). Mice were housed singly in pathogen-free rooms on a 12 h light-dark cycle in shoebox cages modified to include an activity wheel (diameter 30 cm) (Mini Mitter, Sunriver, OR) with *ad libitum* access to drinking water. Mice were monitored daily for signs of morbidity due to the experimental procedure and were removed from the study if they lost 20% of their body weight or had a moribund appearance (ruffled dull fur, hunched posture and abdominal distention). We removed mice from the study if they displayed these signs for >2 days. Mice removed from the study were immediately sacrificed according to protocols established by OHSU Department of Comparative Medicine.

Fatigue, Food Intake and Body Weight Assessment

We used voluntary wheel running activity (VWRA) as an objective proxy for fatigue. We monitored VWRA for each mouse continuously throughout the experimental procedure using the VitalView data acquisition system (Respironics, Sunriver, OR) with an epoch of 60 min. We measured food intake and body weight twice each week (Tuesday and Friday) between 6:00–7:00 a.m. Rodent Diet 5001 (PMI Nutrition International, Brentwood, MO) was placed in the food hopper, and the amount eaten was determined by weighing the food remaining in the hopper. After a two-week acclimation period, each mouse was allowed to establish a 10-day baseline VWRA, after which they were separated into groups. In experiment 1, wild-type mice were divided into two groups. Mice in group 1 (n = 20) received EBRT (as described below) while mice in group 2 (n = 20) were sham irradiated. In experiment 2, wild-type and TNF-α-deficient mice were separated into two groups, respectively (n = 10/group). Wild-type and TNF-α-deficient mice received EBRT as described below while the remaining wild-type and TNF-α-deficient mice were sham irradiated. After treatment mice were returned to their home cages.

Localized External Beam Radiation Therapy

In the first experiment, wild-type C57BL/6 mice received 2.84 Gy/fraction of EBRT to the pelvis five days per week for a total of 24 treatments to a final cumulative dose of 68.2 Gy. The biologically effective dose (BED) for this treatment regimen was 138 for an alpha/beta ratio of 3, which is commonly accepted for prostate cancer. Control mice were sedated in a similar fashion but were not exposed to radiation. Mice were treated between 7:00–8:00 a.m. each morning. Ten mice were placed together in a prone position in an anesthesia chamber and sedated with 5% isoflurane with 4 cc O_2 for 1 min, followed by a maintenance dose of 1.25% isoflurane/4 cc O_2 for 2 min. A 1-cm thick, bolus material was placed over the mice to improve radiation dose distribution, and a Cerrobend™ block was placed over the middle of the field to shield the head and thorax of each mouse. A single anterior field measuring 20 × 23 cm was used to administer 2.84 Gy/fraction of EBRT to the mouse pelvis using 6 MV photons from a clinical linear accelerator (Trilogy™, Varian Medical Systems Inc., Palo Alto, CA). Dosimetry was determined by obtaining a simulation film with the midline Cerrobend block in place to ensure the entire pelvis was in the radiation field, and the head and the thorax were adequately blocked. The radiation dose measured by thermoluminescence dosimetry was within 5% of the calculated dose prescribed to the pelvis and the dose to the head and thorax was less than 0.002 Gy. After irradiation, the isoflurane chamber was immediately flushed with O_2 to remove traces of isoflurane. Mice were allowed to recover in the oxygenated chamber for 4 min at 4 cc/O_2 until they were ambulatory before being returned to their home cages.

In experiment 2, wild-type and TNF-α-deficient mice underwent the same procedure as described above except EBRT-treated wild-type and TNF-α-deficient mice received 4.6 Gy/fraction, 5 days per week for 15 fractions to a total dose of 69 Gy. The BED for this regimen was 83, which is higher than that used clinically but chosen to maximize EBRT-induced effects on fatigue while still being tolerable.

Analysis of Plasma Inflammatory Cytokines and Chemokines

Twenty-four hours after the last treatment, EBRT- and sham-irradiated mice from experiment 1 (n = 10) were terminally sedated, and peripheral blood was immediately collected by direct cardiac puncture and transferred into tubes containing 20 μl of 2 m*M* EDTA and subsequently centrifuged at 13,000 rpm for 6 min in a microcentrifuge. After centrifugation, plasma was removed, aliquoted and immediately stored at −87°C prior to analysis. After collection of peripheral blood, whole brain, spleen, liver and colon were removed and flash frozen in liquid nitrogen prior to quantitative real-time polymerase chain reaction (qRT-PCR) analysis. Plasma inflammatory cytokines and chemokines were measured in duplicate using a bead-based immunofluorescence assay according to the manufacturer's instructions (cat. no. MPXMCYTO70K; EMD Millipore, Billerica, MA). Data were collected and analyzed using the Luminex-100 system Version IS (Luminex® Inc., Austin, TX). A four or five-parameter regression formula was used to calculate the sample concentrations from the standard curves. Relative IL-1β and TNF-α mRNA levels in these tissues were quantified and normalized to GAPDH gene expression using two-step qRT-PCR as described previously (*19*).

Analysis

Daily VWRA was calculated from the number of wheel turns in a 24 h period (12 h light/dark cycle). $VWRA_{base10}$ was calculated as the average daily VWRA for the 10 day period prior to the start of treatment. Repeated analysis of variance (ANOVA) were used to

TABLE 1
Plasma Levels of Inflammatory Analytes in Sham-Irradiated and EBRT-Treated Mice

	Mean ± SD			
Analyte	Control (n = 10)	EBRT (n = 10)	T	*P*
IL-1β	8.4 ± 7.1	10.5 ± 8.5	Ln	0.683
TNF-α	3.2 ± 0.0	6.5 ± 4.1	Ln	0.003[a]
IL-6	24.9 ± 28.9	60.9 ± 98.9	Ln	0.244
IL-1α	102.9 ± 94.3	345.5 ± 503.7	Ln	0.064
MCP-1	22.6 ± 28.4	28.2 ± 24.8	SQRT	0.508
KC	45.1 ± 48.4	91.8 ± 103.0	Ln	0.063
GCSF	215.1 ± 115.3	1734.7 ± 1493.4	Ln	<0.001[a]
IL-9	21.1 ± 29.8	36.7 ± 25.2	Ln	0.065
IP-10	73.6 ± 24.3	121.6 ± 83.3	Ln	0.203

Notes. Plasma inflammatory cytokine and chemokine levels in sham-irradiated mice (control) and EBRT-treated mice sacrificed 24 h after the final sham irradiation or EBRT. The number of animals per group is indicated in parentheses. Mean concentration of each analyte in pg/ml ± standard deviation (SD) is shown. The threshold for detection was 3.2 pg/ml. T = transformation type; Ln = natural log; SQRT = square root.

[a] Statistically significant difference between the groups; $P < 0.006$ was considered statistically significant after Bonferonni correction to control for multiple comparisons.

examine patterns of change in VWRA, body weight and food intake between genotype and treatment group over time. VWRA during the 12 h dark phase was used to calculate dark-phase average time on the wheel, distance run, average speed and peak speed. Total distance was the number of wheel turns in 12 h × circumference of the running wheel (0.942 m); time on wheel was the number of 1 h intervals where wheel rotations were >0, average speed was total distance divided by time on wheel, and peak speed was the maximum speed reached during a 1 h interval. One-way ANOVA was used to determine significant differences between treatment type (EBRT or sham irradiation) at the 95% confidence interval where $P < 0.05$. Repeated ANOVA were used to examine patterns of change in VWRA, food intake and body weight between genotype and/or treatment group. Cytokine C_T values for each sample and primer pair combination and primer efficiency were used to determine fold expression values for IL-1β and TNF-α in EBRT-treated relative to control mice. Gene expression was expressed as fold change relative to the sham-irradiated group using the $2\text{-}\Delta\Delta C_T$ method (*27*). The distribution of all of the inflammatory analytes measured did not follow a normal distribution and therefore transformations were applied. The types of transformations used for each plasma analyte are shown in Table 1. One-way ANOVA was used to determine significant differences between treatment type (EBRT or sham irradiation) at the 95% confidence interval where $P < 0.05$. Data are presented as the mean ± standard error of the mean (SEM) or standard deviation of the mean (SD). $P < 0.05$ was considered to be statistically significant unless *P* values were Bonferroni corrected for multiple comparisons.

RESULTS

Patterns of Change in VWRA, Food Intake and Body Weight in Wild-Type EBRT-Treated Mice

None of the EBRT-treated mice met the criteria for removal from the study based on weight loss or body condition. Figure 1A shows plots of daily VWRA in sham-irradiated (n = 20, closed circle) and EBRT-treated (n = 20, open circle) wild-type mice throughout the 12-day baseline period and treatment week 1–5. VWRA decreased from baseline in both groups at the start of treatment, but VWRA was lower in EBRT-treated mice than in sham-irradiated mice throughout the five weeks of treatment. Figure 1B shows average daily VWRA throughout the baseline period and each of the treatment week 1–5. A time × treatment effect was observed across the five weeks of treatment [$F(5,33) = 9.993$, $P < 0.001$). Figure 1C shows the percentage change from baseline in average dark-phase time on wheel, distance run, average speed and peak speed in EBRT and sham-irradiated mice at the end of the third week of treatment. Compared to sham-irradiated mice, EBRT-treated mice spent less time on their wheels [$F(1,39) = 50.027$, $P < 0.001$], ran a shorter distance [$F(1,39) = 22.374$, $P < 0.001$], at a lower average speed [$F(1,39) = 32.127$, $P < 0.001$] and lower peak speed [$F(1,39) = 22.342$, $P < 0.001$]. Figure 2 shows plots of average body weight and food intake during the baseline and each of the treatment week 1–5. EBRT-treated mice lost body weight during the treatment protocol relative to their sham-irradiated counterparts, whereas sham-irradiated mice gained weight [$F(5,33) = 16.811$, $P < 0.001$]. Statistically significant weight loss in EBRT-treated mice was not apparent until the third week of treatment. The pattern of food intake during treatment was also significantly different between groups [$F(5,33) = 3.584$, $P = 0.011$]. EBRT-treated mice appeared to eat less food during the first week of treatment than the sham-irradiated mice, but intake returned to baseline during subsequent weeks.

EBRT Causes a Systemic Increase in Levels of IL-1β and TNF-α

Twenty-four hours after the final treatment, peripheral blood, liver, spleen, colon and whole brains were collected from 10 mice in each group and IL-1β and TNF-α protein and RNA levels were assessed. Figure 3 shows fold increase in levels of IL-1β and TNF-α mRNA in EBRT-treated mouse tissues relative to sham-irradiated control tissues. Levels of IL-1β were significantly elevated in all tissues, with the exception of whole brain, from EBRT-treated mice relative to controls. TNF-α mRNA levels were significantly

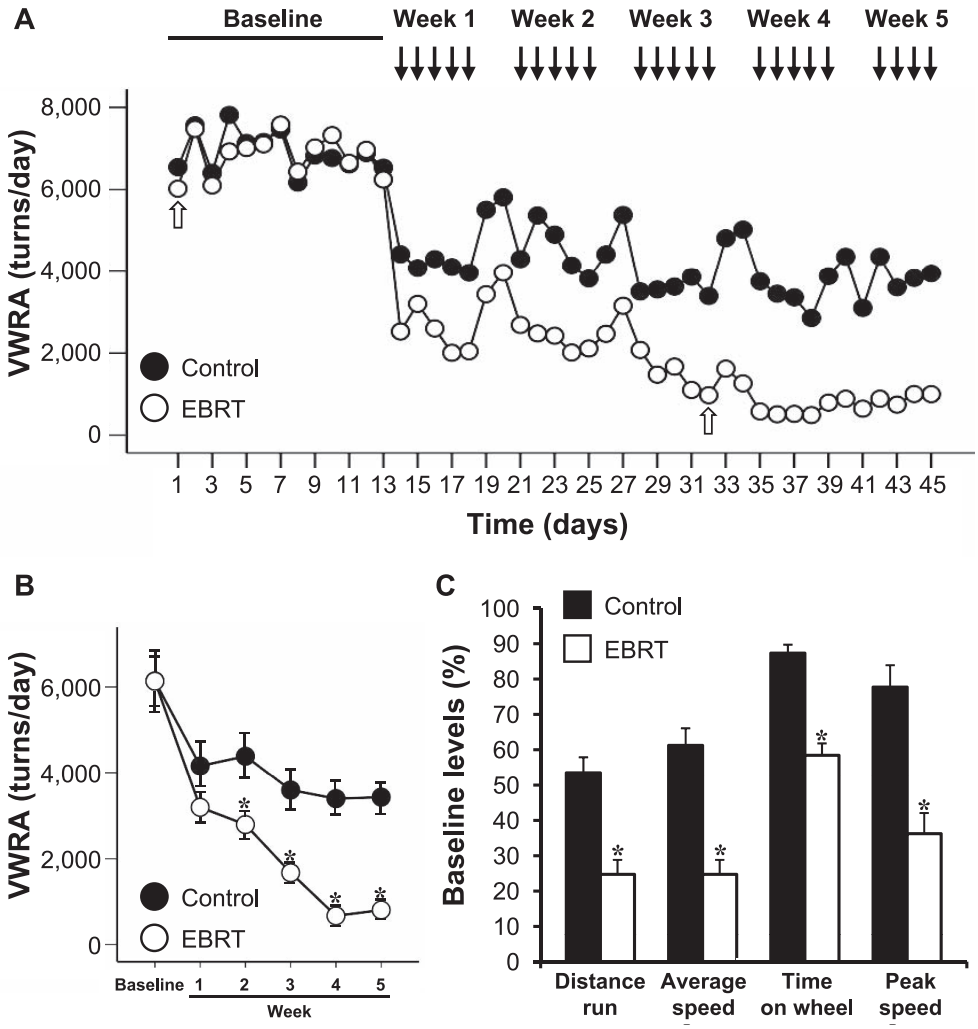

FIG. 1. Fatigue in mice after EBRT to the pelvis. Panel A: Voluntary wheel running activity (VWRA), used as an objective proxy for fatigue, was monitored daily in wild-type C57BL/6 male mice during a 12 day baseline period and then during 24 doses of 2.84 Gy EBRT to the pelvis for a final cumulative radiation dose of 68.2 Gy. Control mice were sedated in a similar fashion but were not exposed to radiation. The filled arrows refer to treatment days. Each data point represents the mean of each value. Error bars are not included in the figure to allow discrimination of data trends. Panel B: Average VWRA during baseline and each week of treatment (week 1–5). Each data point represents the mean ± SEM of each value. Asterisks indicate a statistically significant difference in levels of VWRA between EBRT-treated (open circle) and sham-irradiated (closed circle) mice at each data point ($P < 0.008$, after Bonferroni correction for multiple comparisons). Panel C: Percentage change from baseline (day 1) in dark-phase average distance run, average speed, time on wheel and peak speed calculated on day 32 (see open arrows) in EBRT-treated (open bars) and sham-irradiated (closed bars) mice. Each bar represents the mean ± SEM of each value. Asterisks indicate a statistically significant difference in levels of VWRA between EBRT and sham-irradiated mice ($P < 0.0125$, with Bonferroni correction for multiple comparisons).

elevated in liver, colon and whole brain of EBRT-treated mice relative to control mice. In spleen TNF-α mRNA levels were lower in EBRT-treated mice than in sham-irradiated control mice. Despite elevations in IL-1β mRNA in all tissues examined, plasma IL-1β levels were no different between the two treatment groups (Table 1). In contrast circulating levels of TNF-α were approximately two-fold higher in EBRT-treated mice (Table 1). We also measured plasma levels of IL-1α, granulocyte colony stimulating factor (GCSF), IL-6, keratinocyte chemoattractant (KC), monocyte chemotactic protein 1 (MCP-1), IL-9 and inflammatory protein 10 (IP-10) and observed significant elevations in IL-1α and GCSF (Table 1).

Blockade of TNF-α Signaling has no Effect on EBRT-Induced Fatigue

To determine the specific role of TNF-α in EBRT-induced fatigue, we compared EBRT-induced changes in VWRA in wild-type mice and mice lacking TNF-α. In this

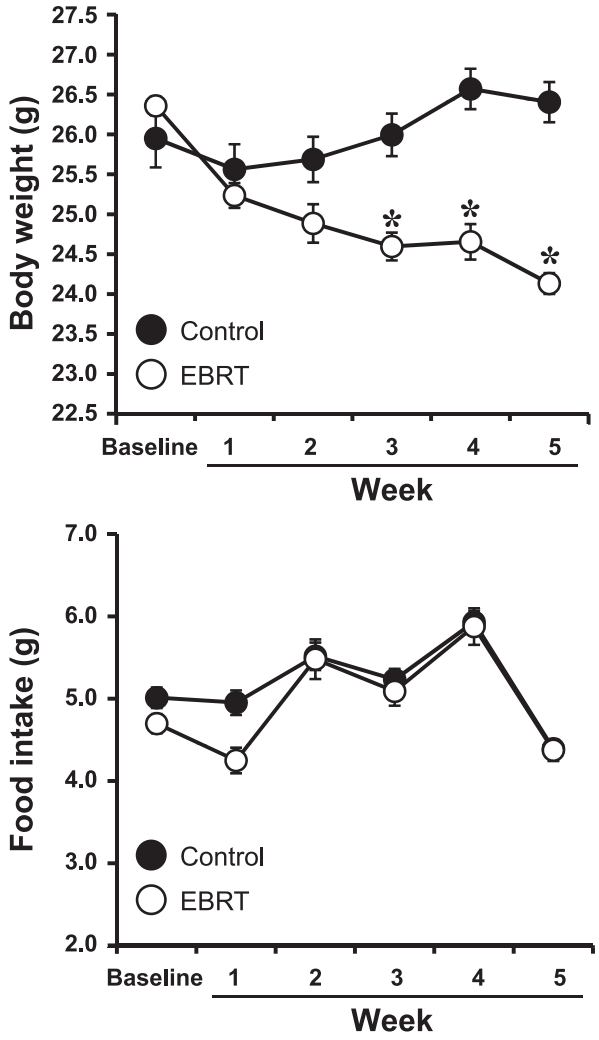

FIG. 2. Weight loss and food intake in mice after EBRT to the pelvis. Average body weight during baseline and each week of treatment (week 1–5). Each data point represents the mean ± SEM of each value. Asterisks indicate a statistically significant difference in levels of VWRA between EBRT-treated (open circle) and sham-irradiated (closed circle) mice ($P < 0.008$, with Bonferroni correction for multiple comparisons).

experiment, we increased the daily dose of EBRT to 4.6 Gy/fraction, five days per week for 15 fractions, for a total dose of 69 Gy. The radiation dose and frequency were tolerable in mice of both genotypes since none of the EBRT-treated mice met the criteria for removal from the study based on weight loss or body condition. Figure 4A shows plots of daily VWRA in EBRT-treated and sham-irradiated mice of both genotypes throughout the 12-day baseline period, each of the treatment week 1–3 and recovery week 4. We observed a similar pattern of decline in VWRA in EBRT-treated mice relative to control mice during the three weeks of treatment, followed by a recovery to baseline during the recovery week (week 4). Figure 4B represents average daily VWRA throughout baseline each of the three treatment weeks (week 1–3) and the recovery week (week 4) as a percentage of baseline. Although there was a significant time × treatment interaction for VWRA [$F(4,32) = 35.224$, $P < 0.001$] no significant time × treatment × genotype effect was observed [$F(4,32) = 1.172$, $P = 0.342$].

Figure 4C–F shows plots of dark-phase average time on wheel, distance run, average speed and peak speed after the tenth treatment and at the end of the recovery week (week 4) expressed as a percentage of baseline. After the tenth treatment wild-type EBRT-treated mice reduced their distance run [$F(1,19) = 20.932$, $P < 0.001$], average speed [$F(1,19) = 12.184$, $P = 0.003$] time on the wheel [$F(1,19) = 19.394$, $P < 0.001$] and peak speed [$F(1,19) = 12.184$, $P = 0.003$]. EBRT-treated TNF-α deficient mice also showed reduced distance run [$F(1,19) = 29.796$, $P < 0.001$], average speed [$F(1,19) = 10.227$, $P = 0.005$] and time on wheel [$F(1,19) = 22.844$, $P < 0.001$] and a near significant decline in peak speed [$F(1,19) = 4.017$, $P = 0.060$] compared to sham-irradiated mice. There was, however, no observed treatment × genotype interaction effect for any of these activity variables at this time point (see Fig. 4 for P values). There was no time × treatment interaction in distance run, average speed, time on wheel or peak speed at the end of the recovery period.

Daily body weight and food intake were also monitored before, during and after treatment. Figure 5 shows plots of average body weight and food intake during baseline and each of the three treatment weeks (week 1–3) and the recovery week (week 4). Similar to VWRA, there was no time × treatment × genotype effect on body weight [$F(4,32) = 2.196$, $P = 0.092$] or food intake [$F(4,32) = 0.076$, $P = 0.989$].

DISCUSSION

Treatment of early-stage prostate cancer involves exposure to fractionated EBRT (2 Gy per dose, five times per week for 8 weeks) for a total cumulative dose of 78 Gy (*1–7*). Men undergoing this treatment regimen frequently report fatigue, which reduces quality of life, physical functioning and long-term overall health (*1–7*). The purpose of this study was to develop a localized EBRT treatment model to facilitate our understanding of the mechanisms underlying EBRT-related fatigue. Our model was similar to the clinical treatment regimen in that the biological equivalent dose of radiation delivered (BED of 138 for an alpha/beta ratio of 3 in experiment 1), is a commonly accepted treatment regimen for prostate cancer. In experiment 2 we used a higher BED than clinical use, for technical feasibility of delivering EBRT and to maximize the potential effects of radiation exposure while still being tolerable in mice. The lack of tumor in our model does not allow for understanding of the interaction between tumor and EBRT on cytokine levels and fatigue.

Using this model we found that EBRT had a cumulative effect on fatigue as evidenced by a progressive decline in VWRA over the course of treatment. To our knowledge this is the first study to examine the relationship between a

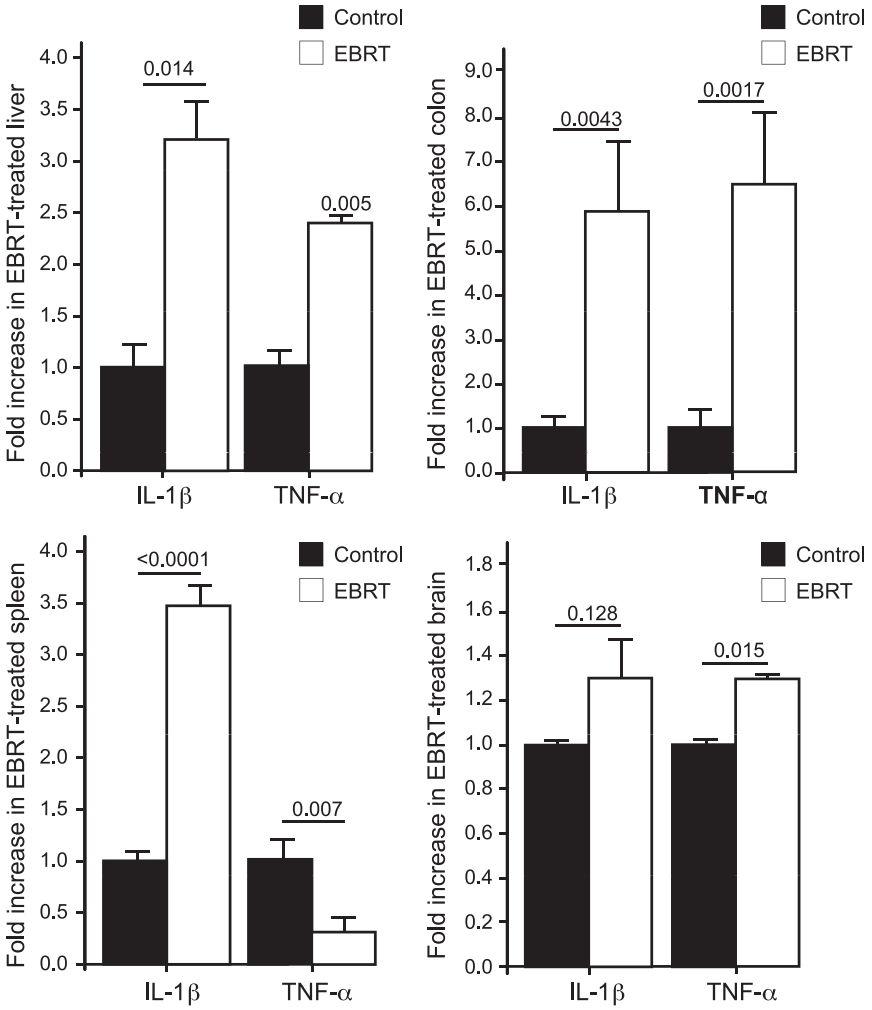

FIG. 3. EBRT induces systemic increases in IL-1β and TNF-α. Fold increase in IL-1β and TNF-α mRNA levels in liver, spleen, colon and whole brain of EBRT-treated mice (open bars) relative to sham-irradiated mice (closed bars) sacrificed 24 h after the final treatment (cumulative dose for EBRT-treated mice was 68.2 Gy). Statistically significant differences in tissue-specific fold increases in mRNA expression levels between groups are indicated by raw *P* values.

clinically relevant localized EBRT, inflammatory cytokines and EBRT-related fatigue in a murine model. By delivering fractionated EBRT over multiple days we were able to administer a clinically relevant radiation dose to the pelvis with minimal toxicity. The reduced toxicity profile was likely due to reduced exposure of highly radiation-sensitive tissues (i.e., gastrointestinal and hematopoietic tissue) to radiation. Prior studies have shown that whole-body irradiation (<20 Gy) in C57BL/6 mice is associated with severe gastrointestinal toxicity and death (*28*). EBRT-treated mice also showed a progressive loss in body weight, which was not associated with a reduction in food intake. We have shown previously the discordance between food intake and weight loss in cancer treatment models. In these models, weight loss may not be driven by reduced caloric intake but cancer treatment-related elevations in inflammatory cytokines. Findings from our recent study support this idea. Using a breast cancer chemotherapy treatment model we found that chemotherapy-induced weight loss was significantly greater in wild-type mice than in mice lacking IL-6, even after controlling for food intake and physical activity level (*29*). EBRT-related fatigue was associated with increased inflammatory gene expression in peripheral tissues and in the circulation. IL-1β expression was elevated in liver, spleen and colon, yet this increase was not associated with similar increases in circulating IL-1β. A similar increase in liver TNF-α mRNA and circulating TNF-α was observed, while TNF-α expression was lower in EBRT-treated spleen and colon. Although it is unclear why TNF-α expression decreased in these tissues our findings support an association between EBRT-induced inflammation and fatigue, suggesting that EBRT-related fatigue may be similar to sickness behavior. Despite the brain being outside of the radiation field we observed a small but significant increase in TNF-α gene expression in whole brain tissue collected from mice 24 h after exposure to

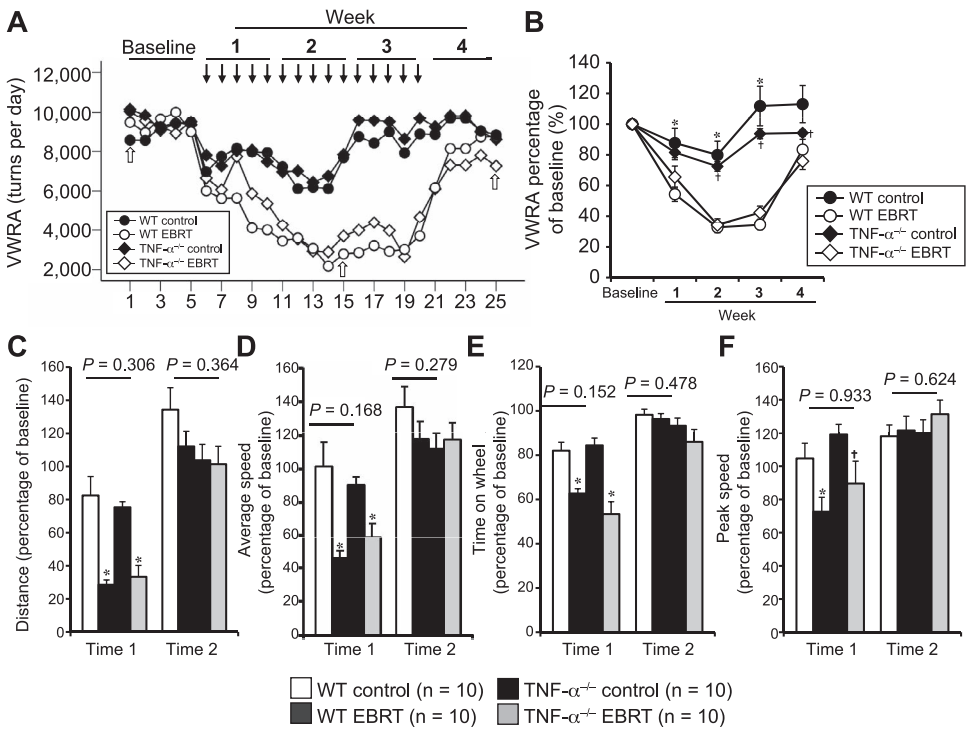

FIG. 4. Blockade of TNF-α signaling has no effect on EBRT-induced fatigue. Panel A: Daily VWRA in EBRT-treated wild-type (open circle) and TNF-α-deficient (open diamond) mice during a 5 day baseline period and then during three weeks of treatment (week 1–3). During each treatment week mice received five daily doses of 4.6 Gy of EBRT to the pelvis for a final cumulative radiation dose of 69 Gy. Monitoring was continued for an additional recovery week post-treatment (week 4). Sham-irradiated wild-type (closed circle) and TNF-α-deficient (closed diamond) mice were treated identically but were not exposed to EBRT. Nontreatment days (i.e., weekends) are not shown. Error bars and other markers are not included to allow for discrimination of data trends. Panel B: Average VWRA during baseline and for each treatment week (week 1–3) and the recovery week (week 4) as a percentage of baseline. Each data point represents the mean ± SEM of each value. Statistically significant difference in levels of VWRA between EBRT-treated and sham-irradiated mice are denoted by (*) for wild-type mice and (†) for TNF-α-deficient mice. $P < 0.0125$ was considered statistically significant after Bonferroni correction for multiple comparisons. Panels C–F: Percentage changes from baseline (day 1) in distance run (panel C), average speed (panel D), time on wheel (panel E) and peak speed (panel F) were calculated after the tenth treatment (time 1; day 15) and the last day of the recovery period (time 2; day 25). Two-way ANOVA was used to detect significant treatment × genotype interactions (see underlined P values above each bar cluster). Each bar represents the mean ± SEM of each value. *$P < 0.05$, s$P = 0.060$, for comparison between treatment groups within genotypes.

fractionated radiation up to 72 Gy. Our results are similar to those of Marquette *et al*. who showed that a single high dose (15 Gy) of total-body irradiation with the head shielded increased IL-1β, TNF-α and IL-6 gene expression in rat brains (*30*). These authors found that vagal nerve afferents played a central role in communicating peripheral inflammatory signals to the brain since radiation-induced brain inflammation was dampened in vagotomized animals.

Despite the observed association between EBRT-induced fatigue and systemic inflammation, patterns of fatigue were no different between TNF-α deficient mice and their wild-type counterparts. This finding may suggest that TNF-α does not play a key role in EBRT-related fatigue. An alternate explanation is that in the absence of TNF-α, other inflammatory cytokines can compensate for the lack of TNF-α in this model. IL-1β is one candidate since prior studies have demonstrated synergism between these two cytokines in the induction of systemic inflammation and sickness behavior (*19, 31*). Similar experiments in mice lacking both IL-1β and TNF-α signaling pathway may shed light on the synergistic action of these cytokines in EBRT-induced fatigue. In a prior study we used this approach to examine the role of IL-1β and TNF-α signaling in chemotherapy related fatigue. While blockade of IL-1β and TNF-α signaling dampened the systemic inflammatory response to cytotoxic chemotherapy it also decreased survival (*19*). Thus, it is possible that EBRT-related toxicities may be enhanced in doubly cytokine-deficient mice. In addition to further examining the specific role of inflammatory cytokines and chemokines in EBRT-related fatigue, this model could be used to investigate the neural mechanisms of EBRT-related fatigue. In mouse models of sickness behavior and cancer chemotherapy-related fatigue, acute lethargy after endotoxin or chemotherapy administra-

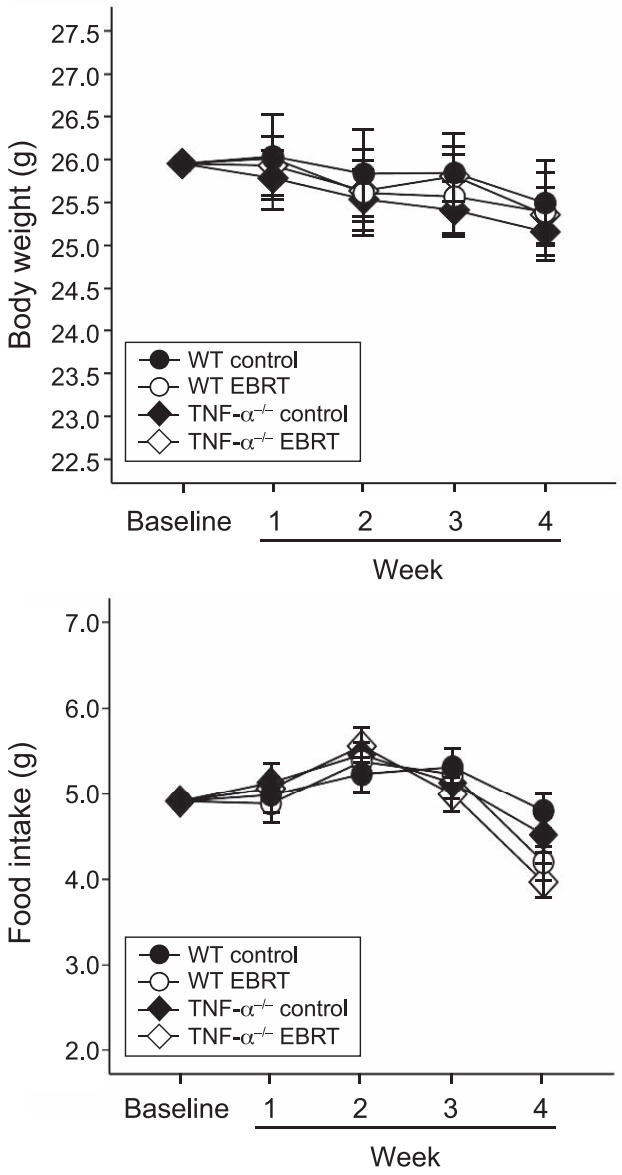

FIG. 5. Blockade of TNF-α signaling has no effect on EBRT-induced body weight or food intake. Average body weight during baseline and each week of treatment (week 1–3) and the recovery week (week 4). Each data point represents the mean ± SEM of each value.

tion is caused by hypofunction of a population of inflammation-responsive hypothalamic neurons (*16, 32*). These neurons secrete the neurotransmitter orexin, which regulates sleep-wake cycles. It is possible that localized EBRT could be having a similar effect on orexin neurons to mediate EBRT-related fatigue. Additional experiments are warranted to determine whether this is the case.

ACKNOWLEDGMENTS

We would like to thank Daniel Roberts and Xiao Yue Han of Oregon Health and Science University for assistance with the RT-PCR experiments and the animal work. Funding for this study was provided by the National Institute for Nursing Research (no. R21NR010363) to LJW.

Received: March 3, 2015; accepted: October 9, 2015; published online: 00 00, 00

REFERENCES

1. Fransson P. Fatigue in prostate cancer patients treated with external beam radiotherapy: a prospective 5-year long-term patient-reported evaluation. J Cancer Res Ther 2010; 6:516–20.
2. Fransson P, Damber JE, Widmark A. Health-related quality of life 10 years after external beam radiotherapy or watchful waiting in patients with localized prostate cancer. Scand J Urol Nephrol 2009; 43:119–26.
3. Geinitz H, Thamm R, Scholz C, Heinrich C, Prause N, Kerndl S, et al. Longitudinal analysis of quality of life in patients receiving conformal radiation therapy for prostate cancer. Strahlenther Onkol 2010; 186:46–52.
4. Miaskowski C, Paul SM, Cooper BA, Lee K, Dodd M, West C, et al. Trajectories of fatigue in men with prostate cancer before, during, and after radiation therapy. J Pain Symptom Manage 2008; 35:632–43.
5. Monga U, Kerrigan AJ, Thornby J, Monga TN, Zimmermann KP. Longitudinal study of quality of life in patients with localized prostate cancer undergoing radiotherapy. J Rehabil Res Dev 2005; 42:391–9.
6. Talcott JA, Manola J, Clark JA, Kaplan I, Beard CJ, Mitchell SP, et al. Time course and predictors of symptoms after primary prostate cancer therapy. J Clin Oncol 2003; 21:3979–86.
7. Vordermark D, Schwab M, Flentje M, Sailer M, Kolbl O. Chronic fatigue after radiotherapy for carcinoma of the prostate: correlation with anorectal and genitourinary function. Radiother Oncol 2002; 62:293–7.
8. Danjoux C, Gardner S, Fitch M. Prospective evaluation of fatigue during a course of curative radiotherapy for localised prostate cancer. Support Care Cancer 2007; 15:1169–76.
9. Storey DJ, McLaren DB, Atkinson MA, Butcher I, Liggatt S, O'Dea R, et al. Clinically relevant fatigue in recurrence-free prostate cancer survivors. Ann Oncol 2012; 23:65–72.
10. Beard CJ, Propert KJ, Rieker PP, Clark JA, Kaplan I, Kantoff PW, et al. Complications after treatment with external-beam irradiation in early-stage prostate cancer patients: a prospective multiinstitutional outcomes study. J Clin Oncol 1997; 15:223–9.
11. Maliski SL, Kwan L, Orecklin JR, Saigal CS, Litwin MS. Predictors of fatigue after treatment for prostate cancer. Urology 2005; 65:101–8.
12. Davidovich P, Kearney CJ, Martin SJ. Inflammatory outcomes of apoptosis, necrosis and necroptosis. Biol Chem 2014; 395:1163–71.
13. Hart BL. Biological basis of the behavior of sick animals. Neurosci Biobehav Rev 1988; 12:123–37.
14. Dantzer R. Cytokine, sickness behavior, and depression. Immunol Allergy Clin North Am 2009; 29:247–64.
15. Skinner GW, Mitchell D, Harden LM. Avoidance of physical activity is a sensitive indicator of illness. Physiol Behav 2009; 96:421–7.
16. Grossberg AJ, Zhu X, Leinninger GM, Levasseur PR, Braun TP, Myers MG,Jr, et al. Inflammation-induced lethargy is mediated by suppression of orexin neuron activity. J Neurosci 2011; 31:11376–86.
17. Weymann KB, Wood LJ, Zhu X, Marks DL. A role for orexin in cytotoxic chemotherapy-induced fatigue. Brain Behav Immun 2013; 37:84–94.
18. Wood LJ, Nail LM, Perrin NA, Elsea CR, Fischer A, Druker BJ. The cancer chemotherapy drug etoposide (VP-16) induces pro-inflammatory cytokine production and sickness behavior-like

symptoms in a mouse model of cancer chemotherapy related symptoms. Biol Res Nurs 2006; 7:157–69.

19. Smith LB, Leo MC, Anderson C, Wright TJ, Weymann KB, Wood LJ. The role of IL-1beta and TNF-alpha signaling in the genesis of cancer treatment related symptoms (CTRS): A study using cytokine receptor-deficient mice. Brain Behav Immun. 2014; 38:66–76.

20. Mahoney SE, Davis JM, Murphy EA, McClellan JL, Gordon B, Pena MM. Effects of 5-fluorouracil chemotherapy on fatigue: role of MCP-1. Brain Behav Immun 2013; 27:155–61.

21. Ray MA, Trammell RA, Verhulst S, Ran S, Toth LA. Development of a mouse model for assessing fatigue during chemotherapy. Comp Med 2011; 61:119–30.

22. Cleeland CS, Bennett GJ, Dantzer R, Dougherty PM, Dunn AJ, Meyers CA, et al. Are the symptoms of cancer and cancer treatment due to a shared biologic mechanism? A cytokine-immunologic model of cancer symptoms. Cancer 2003; 97:2919–25.

23. Kovacs CJ, Daly BM, Evans MJ, Johnke RM, Lee TK, Karlsson UL, et al. Cytokine profiles in patients receiving wide-field + prostate boost radiotherapy (xRT) for adenocarcinoma of the prostate. Cytokine 2003; 23:151–63.

24. Greenberg DB, Gray JL, Mannix CM, Eisenthal S, Carey M. Treatment-related fatigue and serum interleukin-1 levels in patients during external beam irradiation for prostate cancer. J Pain Symptom Manage 1993; 8:196–200.

25. Dirksen SR, Kirschner KF, Belyea MJ. Association of symptoms and cytokines in prostate cancer patients receiving radiation treatment. Biol Res Nurs 2013; 16:250–7.

26. Alexopoulou L, Kranidioti K, Xanthoulea S, Denis M, Kotanidou A, Douni E, et al. Transmembrane TNF protects mutant mice against intracellular bacterial infections, chronic inflammation and autoimmunity. Eur J Immunol 2006; 36:2768–80.

27. Livak KJ, Schmittgen TD. Analysis of relative gene expression data using real-time quantitative PCR and the 2(-Delta Delta C(T)) method. Methods 2001; 25:402–8.

28. Qiu W, Leibowitz B, Zhang L, Yu J. Growth factors protect intestinal stem cells from radiation-induced apoptosis by suppressing PUMA through the PI3K/AKT/p53 axis. Oncogene 2010; 29:1622–32.

29. Elsea CR, Kneiss JA, Wood LJ. Induction of IL-6 by cytotoxic chemotherapy is associated with loss of lean body and fat mass in tumor-free female mice. Biol Res Nurs 2015; 17:549–57.

30. Marquette C, Linard C, Galonnier M, Van Uye A, Mathieu J, Gourmelon P, et al. IL-1beta, TNFalpha and IL-6 induction in the rat brain after partial-body irradiation: role of vagal afferents. Int J Radiat Biol 2003; 79:777–85.

31. Bluthe RM, Laye S, Michaud B, Combe C, Dantzer R, Parnet P. Role of interleukin-1beta and tumour necrosis factor-alpha in lipopolysaccharide-induced sickness behaviour: a study with interleukin-1 type I receptor-deficient mice. Eur J Neurosci 2000; 12:4447–56.

32. Weymann KB, Wood LJ, Zhu X, Marks DL. A role for orexin in cytotoxic chemotherapy-induced fatigue. Brain Behav Immun 2014; 37:84–94.